Planck Spectroscopy and Quantum Noise of Microwave Beam Splitters

M. Mariantoni,[1,2,*] E. P. Menzel,[1,2] F. Deppe,[1,2] M. Á. Araque Caballero,[1,2] A. Baust,[1,2] T. Niemczyk,[1,2] E. Hoffmann,[1,2] E. Solano,[3,4] A. Marx,[1] and R. Gross[1,2,†]

[1]*Walther-Meißner-Institut, Bayerische Akademie der Wissenschaften, D-85748 Garching, Germany*
[2]*Physik-Department, Technische Universität München, D-85748 Garching, Germany*
[3]*Departamento de Química Física, Universidad del País Vasco-Euskal Herriko Unibertsitatea, 48080 Bilbao, Spain*
[4]*IKERBASQUE, Basque Foundation for Science, Alameda Urquijo 36, 48011 Bilbao, Spain*

(Received 16 March 2010; published 20 September 2010)

We use a correlation function analysis of the field quadratures to characterize both the blackbody radiation emitted by a 50 Ω load resistor and the quantum properties of two types of beam splitters in the microwave regime. To this end, we first study vacuum fluctuations as a function of frequency in a Planck spectroscopy experiment and then measure the covariance matrix of weak thermal states. Our results provide direct experimental evidence that vacuum fluctuations represent the fundamental minimum quantum noise added by a beam splitter to any given input signal.

DOI: 10.1103/PhysRevLett.105.133601 PACS numbers: 42.50.Lc, 07.57.−c, 42.79.Fm

At optical frequencies, single-photon detectors [1] and beam splitters are key ingredients for realizing quantum optics experiments. These devices are crucial for the implementation of quantum homodyne tomography [2] and quantum information processing and communication [3], as well as all-optical quantum computing [4]. The recent advent of circuit quantum electrodynamics [5–15] has paved the way for the generation of single photons in the microwave (mw) regime [11,15]. Despite the rapid advances in this field, the availability of mw photodetectors [16,17] and well-characterized mw beam splitters is still at an early stage. However, we have recently shown that the use of low-noise cryogenic high electron mobility transistor (HEMT) amplifiers represents a versatile approach for the analysis of mw signals on a single-photon level. Although the phase-insensitive HEMT amplifiers obscure the signal by adding random noise of typically 10–20 photons at 5 GHz, they do not perturb the correlations of signals opportunely split into two parts and then processed by two parallel amplification and detection chains. In such a setup, a correlation analysis allows for full state tomography of propagating quantum mw signals and the detector noise, simultaneously [18]. We note that HEMT amplifiers represent available ''off-the-shelf'' technology and offer flat gain over a broad frequency range of several gigahertz. Here, we present results of two experiments demonstrating the successful application of our setup to the characterization of weak thermal states. In a first experiment denoted as Planck spectroscopy, we analyze the mw blackbody radiation emitted by a matched 50 Ω load resistor as a function of temperature in the frequency regime $4.7 \leq \omega/2\pi \leq 7.1$ GHz. Besides confirming that the mean thermal photon number follows Bose-Einstein statistics [19–22], our data directly show that the quantum crossover temperature T_{cr} shifts with frequency as $T_{\mathrm{cr}} = \hbar\omega/2k_B$, providing an indirect measure of mw vacuum fluctuations with high fidelity. In a second experiment, we use weak thermal states for a detailed experimental characterization of mw beam splitters at the quantum level. This task is particularly important because mw beam splitters are key elements in a variety of quantum-optical experiments such as Mach-Zehnder and Hanbury Brown–Twiss interferometry [1,19].

The experimental setup is shown in Fig. 1. As an ideal blackbody source emitting thermal mw states [23], we use matched 50 Ω loads whose temperature T can be varied between 20 and 350 mK and measured with a RuO thermometer. The associated quantum voltage is

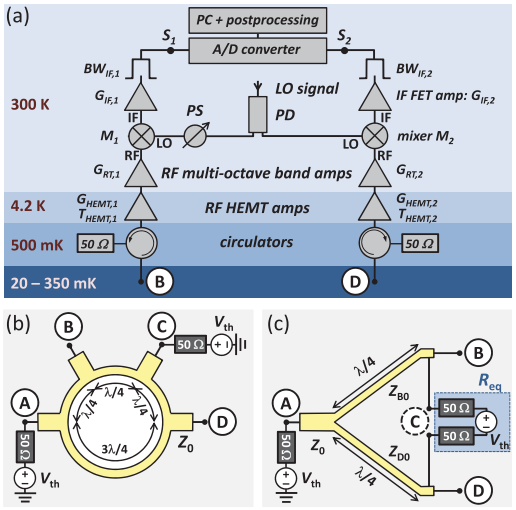

FIG. 1 (color). Schematics of the experimental setup. (a) Amplification and detection chains. (b) 180° HR. (c) WPD. For the WPD, port C represents a hidden internal port and R_{eq} an internal distributed resistor, which can be modeled as two matched 50 Ω loads adding correlated thermal noise via the hidden port C only.

$\hat{V}_{\rm th} = V_0(\hat{p}^\dagger + \hat{p})$, where $V_0^2 = 4 \times {\rm BW} \times R_0\hbar\omega/2$, where $R_0 = 50\ \Omega$, $\hat{p}^\dagger$ and $\hat{p}$ are bosonic creation and annihilation operators, respectively, and BW is the bandwidth. The thermal mw signal is fed to the input ports of a 3 dB mw beam splitter. We perform experiments on two different beam splitter realizations: a four-port 180° hybrid ring (HR) [cf. Fig. 1(b)] and a three-port Wilkinson power divider (WPD) [cf. Fig. 1(c)]. For the WPD, an internal distributed resistor $R_{\rm eq}$ shunting the output ports B and D provides isolation between those ports and impedance matching for port A. In addition, an external 50 Ω load is attached to input port A. For the HR, matched 50 Ω loads are attached to both input ports A and C. The input-output relations of the HR are $\hat{V}_{\rm B} = (\hat{V}_{\rm A} + \hat{V}_{\rm C})/\sqrt{2}$ and $\hat{V}_{\rm D} = (-\hat{V}_{\rm A} + \hat{V}_{\rm C})/\sqrt{2}$ [24]. We remark that the WPD, although appearing to be a three-port device, has to be treated quantum mechanically as having an additional ''hidden'' internal fourth port C [see Fig. 1(c)], ensuring energy conservation and commutation relations. In this case the input-output relations are $\hat{V}_{\rm B} = (\hat{V}_{\rm A} - \hat{V}_{\rm C})/\sqrt{2}$ and $\hat{V}_{\rm D} = (\hat{V}_{\rm A} + \hat{V}_{\rm C})/\sqrt{2}$. Regarding thermal noise, the internal resistor $R_{\rm eq}$ can be modeled as two equivalent matched 50 Ω loads. The noise added by these thermal noise sources in the two arms acts as if it were correlated. If the input signal at port A is large, this additional noise can be neglected and the WPD can be treated as a three-port device.

As shown in Fig. 1(a), the output ports B and D of the beam splitter are connected to two symmetric amplification and detection chains, each comprising: (i) a cryogenic circulator at 500 mK with 21 dB isolation which prevents amplifier noise from leaking back to the mw source under study. Furthermore, together with the isolation between two outputs of the beam splitters they avoid spurious correlations of the noise originating from the two amplification chains. (ii) A low-noise HEMT amplifier thermally anchored at 4.2 K with power gain $G_{\rm HEMT} \simeq 24$ dB and noise temperature $T_{\rm HEMT} \simeq 6 \pm 1$ K. The noise added by the linear HEMT amplifiers is the dominating amplifier noise in each detection channel and is expressed by $\hat{\chi} = V_0(\hat{\xi}^\dagger + \hat{\xi})$, where $\hat{\xi}^\dagger$ and $\hat{\xi}$ are bosonic creation and annihilation operators, respectively [25]. (iii) A room-temperature amplifier and (iv) a mixer (M) and local oscillator (LO) to down-convert the mw signal to the intermediate frequency (IF). The phase $\varphi_{\rm LO}$ of one of the two LO signals obtained by means of a power divider (PD) can be varied by a phase shifter (PS). (v) An IF amplifier and (vi) a 7 kHz to 26 MHz bandpass filter. By using a double sideband receiver the total bandwidth in our experiment is twice the bandwidth of the bandpass filter. The down-converted voltage signals s_1 and s_2 in the two chains are finally synchronously digitized by an acquisition board with 4×10^8 samples/s and 12 bit resolution.

According to Nyquist [26], the blackbody radiation emitted by a resistor R_0 within the BW around the frequency $\omega = \omega_{\rm LO}$ is given by $\langle V_{\rm th}^2\rangle/R_0 = 4 \times {\rm BW} \times \langle n_{\rm th}\rangle\hbar\omega$. Here, $\langle n_{\rm th}\rangle$ is the average thermal photon population. It has been shown that for conductors with a large number of electronic modes the statistics of the emitted photons is given by a Bose-Einstein distribution [23]. In this case the well-known result $\langle V_{\rm th}^2\rangle/R_0 = 4 \times {\rm BW} \times \frac{\hbar\omega}{2}\coth(\hbar\omega/2k_BT)$ is obtained. The power emitted into a matched circuit with characteristic impedance Z_0 is reduced by a factor of 1/4 due to voltage division. Together with the beam splitter input-output relations of the HR, the signal components s_1 and s_2 are given by $s_1 = \sqrt{G_1}(\alpha V_{\rm th}^{\rm A} + \beta V_{\rm th}^{\rm C} + \chi_1)$ and $s_2 = \sqrt{G_2}(-\alpha V_{\rm th}^{\rm A} + \beta V_{\rm th}^{\rm C} + \chi_2)$. Here, $G_1 \simeq G_2$ is the total power gain of the amplification chains, $\alpha = \beta = 1/2\sqrt{2}$, and χ_1 and χ_2 are the independent noise contributions of the amplifiers. Equivalently, for the WPD we obtain $s_1 = \sqrt{G_1}(\alpha V_{\rm th}^{\rm A} - \beta V_{\rm th}^{\rm C} + \chi_1)$ and $s_2 = \sqrt{G_2}(\alpha V_{\rm th}^{\rm A} + \beta V_{\rm th}^{\rm C} + \chi_2)$. We note that $V_{\rm th}^{\rm A}$, $V_{\rm th}^{\rm C}$, and $\chi_{1,2}$ are classical realizations of the operators given above. By recording a large number of 1 μs-long time traces ($\sim 10^6$), the auto- and cross-correlation functions $R_{ii}(\tau) = \langle s_i^*(t+\tau)s_i(t)\rangle/Z_0 = \sigma_{ii}^2{\rm sinc}({\rm BW} \times \tau)/Z_0$ and $R_{ij}(\tau) = \langle s_i^*(t+\tau)s_j(t)\rangle/Z_0 = \sigma_{ij}^2{\rm sinc}({\rm BW} \times \tau)\cos\varphi_{\rm LO}/Z_0$, respectively, can be calculated ($i, j = 1, 2$). Since $\langle s_i(t)\rangle = 0$ for thermal states, the auto- and cross-correlation functions are equal to the autovariance $C_{ii}(\tau) = R_{ii}(\tau) - \langle s_i\rangle^2$ and cross-variance $C_{ij}(\tau) = R_{ij}(\tau) - \langle s_i\rangle\langle s_j\rangle$, respectively. Here, τ is the time shift between two traces being correlated, and σ_{ii}^2 and σ_{ij}^2 are the variance and covariance, respectively, of the voltage signals s_1 and s_2.

We first discuss the Planck spectroscopy experiment [21,22]. Here, we use only a single amplification chain and determine the autocorrelation function $R_{11}(\tau)$ or $R_{22}(\tau)$. Figure 2(a) shows the measured $R_{11}(\tau)$ obtained for $T = 30$ mK by using a WPD. A similar result is obtained for $R_{22}(\tau)$ [see Fig. 3(d)]. Fitting the data to $C_{11}(\tau)$ allows us to extract the measurement bandwidth BW $\simeq$ 52 MHz. Assuming that the signal contributions $V_{\rm th}^{\rm A}$ and $V_{\rm th}^{\rm C}$ due to the two load resistors and the noise χ_i of the HEMT amplifier are independent, we can add up their variances and obtain $R_{ii}(0) = C_{ii}(0) = \sigma_{ii}^2 = \langle s_i^2\rangle/Z_0 = \frac{G_i}{Z_0}[(\alpha^2 + \beta^2)\langle V_{\rm th}^2\rangle + \langle\chi_i^2\rangle]$. With $\hbar\omega/2k_BT_{\rm HEMT} \ll 1$ we can introduce a classical noise temperature $T_{i,{\rm HEMT}}$ for the amplifiers and obtain

$$R_{ii}(0) = G_i^\star \times {\rm BW} \times \left[\frac{\hbar\omega}{2}\coth\frac{\hbar\omega}{2k_BT} + k_BT_{i,{\rm HEMT}}^\star\right]. \quad (1)$$

Here, $G_i^\star = \gamma G_i$ is the effective gain with G_i the total gain of the amplification chain and $T_{i,{\rm HEMT}}^\star = T_{i,{\rm HEMT}}/\gamma$ is the amplifier effective noise temperature, representing the amplifier noise temperature relative to the input of the WPD. For both HR and WPD, $\gamma = 4(\alpha^2 + \beta^2) = 1$.

Figure 2(b) shows the measured variance $R_{11}(0)$ as a function of T for $\omega/2\pi = 5.3$ GHz in the case of a WPD. In the experiments, T was varied between 20 and 350 mK by means of a resistive heater and continuously monitored with a RuO thermometer. The measured variance is close

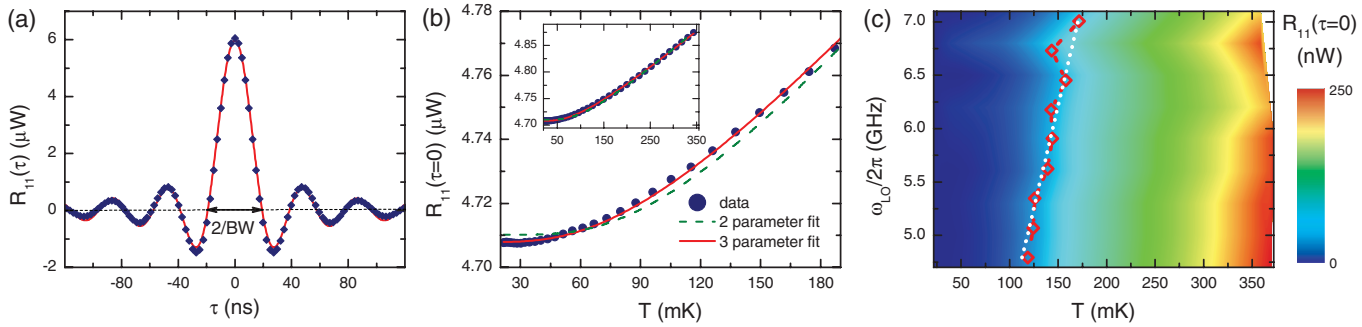

FIG. 2 (color). Planck spectroscopy of thermal mw states at $\omega/2\pi = 5.3$ GHz using a WPD. (a) Autocorrelation function $R_{11}(\tau)$. The line is a fit to the data (symbols). (b) Temperature dependence of the variance $R_{11}(\tau = 0)$ (Planck function). The dashed and full lines are obtained by two and three parameter fits, respectively, to the data (symbols). Inset: Wider T range. (c) Planck spectroscopy. Contour plot of $R_{11}(\tau = 0)$ versus T for different $\omega/2\pi$. The data have been corrected for the frequency-dependent amplifier gain, and the offset due to vacuum and amplifier noise has been subtracted. Symbols and dotted line: Measured and expected quantum crossover temperatures $T_{\rm cr} = \hbar\omega/2k_B$, respectively.

to a Planck function and reproduces the quantum crossover at $T_{\rm cr} = \hbar\omega/2k_B$. A fit of Eq. (1) to the data using $G_1^\star$ and $T_{1,\rm HEMT}^\star$ as free parameters yields $G_1^\star \simeq 90$ dB and $T_{1,\rm HEMT}^\star \simeq 6$ K. The slight deviations between the data and the two-parameter fit can be understood by taking into account that the effective electronic temperature $T_{\rm eff}$ of the load resistors at ports A and C may differ by a small amount δT. By using δT as the third fitting parameter, the solid line in Fig. 2(b) is obtained, demonstrating excellent agreement with the experimental data. The δT values obtained by fitting the data are reasonably small and typically range between 1 and 10 mK. The large bandwidth of the HEMT amplifier allows us to perform equivalent measurements at several frequencies between 4.7 and 7.1 GHz. The result of such Planck spectroscopy is shown in Fig. 2(c). Clearly, the quantum crossover temperature $T_{\rm cr}$ shifts to higher values with increasing frequency. Because of the finite uncertainty in $T_{\rm eff}$, we derive an effective crossover temperature $T_{\rm cr} + \delta T_{\rm cr}$, which again slightly deviates from the theoretically expected value [cf. Fig. 2(c)]. The magnitude $\delta T_{\rm cr}$ quantifies the measurement fidelity $\mathcal{F} \equiv 1 - |\delta T_{\rm cr}|/T_{\rm cr}$ of our setup for vacuum fluctuations. Notably, for the entire frequency range $\mathcal{F} \gtrsim 95\%$. In summary, our Planck spectroscopy experiments not only provide clear evidence for the Bose-Einstein statistics of photons emitted by a conductor in the few photon limit, but also directly demonstrate the frequency dependence of the quantum crossover temperature.

We next turn to the analysis of the mw beam splitters. Figures 3(a)–3(d) show the entire correlation matrix. The off-diagonal elements are cross-correlation functions measured by choosing $\varphi_{\rm LO}$ in order to obtain a maximum positive result. This guarantees that the signals associated with the two detection channels are skewed in phase and no unwanted decorrelation is introduced. Since the signal contributions of the thermal noise sources and the amplifier

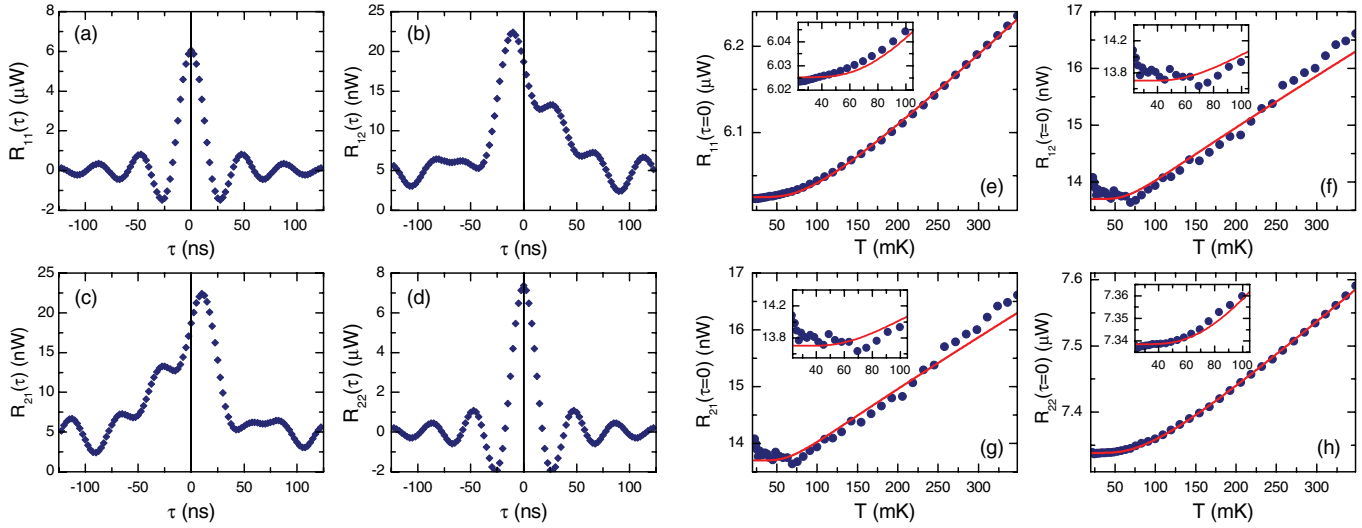

FIG. 3 (color). Full correlation function and covariance matrices measured at $\omega/2\pi = 5.0$ GHz using a WPD ($G_1 \simeq 90.5$ dB, $G_2 \simeq 91.3$ dB, and $G_{12} \simeq 90.9$ dB). (a)–(d) $R_{ii}(\tau)$ and $R_{ij}(\tau)$ measured at $T = 30$ mK. (e)–(h) Temperature dependence of $R_{ii}(0)$ and $R_{ij}(0)$. The lines are fits to the data (symbols) including a global offset of about 0.2 photons in the measurement bandwidth.

noise are independent, all cross correlations vanish, e.g., $\langle \hat{\chi}_1 \hat{\chi}_2 \rangle = \langle \hat{\chi}_1 \rangle \langle \hat{\chi}_2 \rangle = 0$. Then, for $\alpha^2 = \beta^2 = 1/8$ the covariance $R_{12}(0) = C_{12}(0) = \sigma_{12}^2$ is obtained to

$$R_{12}(0) = \frac{\hbar\omega}{4} G_{12} \times \mathrm{BW} \times \left[\coth\frac{\hbar\omega}{2k_B T_\mathrm{A}} - \coth\frac{\hbar\omega}{2k_B T_\mathrm{C}} \right] \quad (2)$$

with the power cogain $G_{12} = \sqrt{G_1}\sqrt{G_2}$. We note that the temperatures T_A and T_C of the load resistors at ports A and C, respectively, are identical only in the ideal case, resulting in $R_{12}(0) = 0$ for the HR and WPD. However, in real experiments the temperatures differ slightly: $T_\mathrm{A} = T_\mathrm{C}(1 - \eta)$. Figures 3(e)–3(h) show the covariance matrix as a function of T for $\omega/2\pi = 5.0$ GHz and using a WPD. The diagonal matrix elements $R_{11}(0)$ and $R_{22}(0)$ represent variance measurements and are analogous to the results of Fig. 2(b). The off-diagonal elements, instead, represent covariance measurements. It is evident that both the offset signal at 20 mK and the signal span between 20 and 350 mK for the covariance is reduced by about 2 orders of magnitude as compared to the variance. This suggests that there is a cancellation of both the amplifier noise and the signal when measuring the covariance. The former is due to the fact that the amplifier noises are uncorrelated. The latter is expected from Eq. (2). In order to prove this conjecture, we use Eq. (2) to fit the experimental data by using the cogain determined from the variance data. Furthermore, we set $T_\mathrm{A} = T$, where T is the temperature measured by the thermometer, and use η as a free fitting parameter. We thus obtain the red curves in Figs. 3(f) and 3(g), which are in excellent agreement with the data. We obtain η values of less than 2% amounting to temperature differences of a few mK. Since Eq. (2) explicitly assumes the existence of four ports, the perfect fit of the experimental data provides clear evidence that the WPD effectively behaves as a four-port device. In the quantum limit, this fourth port adds vacuum noise to any given input signal. In order to confirm our findings on the WPD, we have measured the T dependence of the variance and covariance also for a HR (cf. Fig. 4), which is a straightforward four-port beam splitter. The covariance data of Fig. 4(b) are in very good agreement with the fitted curve obtained from Eq. (2). This clearly demonstrates that both the HR and WPD are characterized by the same fundamental quantum-mechanical behavior.

In conclusion, we have applied a correlation function analysis of the field quadratures to characterize blackbody radiation and the quantum properties of mw beam splitters. Our Planck spectroscopy experiments show that the mean thermal photon number emitted by a load resistor follows Bose-Einstein statistics and that the quantum crossover temperature shifts with frequency as $T_\mathrm{cr} = \hbar\omega/2k_B$, providing an indirect measure of mw vacuum fluctuations with high fidelity. Moreover, we have shown that, at the quantum level, even seemingly three-port beam splitters are actual four-port devices adding at least the vacuum noise to any input signal.

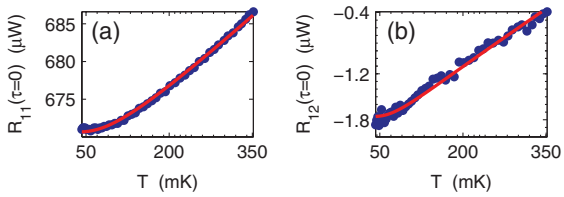

FIG. 4 (color). Temperature dependence of the (a) variance $R_{11}(0)$ and (b) covariance $R_{12}(0)$ measured at $\omega/2\pi = 5.85$ GHz using a HR. The different power scale compared to Figs. 3(e)–3(h) results from a different amplifier configuration.

This work is supported by the German Research Foundation through SFB 631, the German Excellence Initiative via NIM, Basque Government Grant No. IT472-10, Spanish MICINN Project No. FIS2009-12773-C02-01, and the SOLID European project.

*Present address: Department of Physics, University of California, Santa Barbara, CA 93106, USA. matmar@physics.ucsb.edu

†Rudolf.Gross@wmi.badw.de

[1] L. Mandel and E. Wolf, *Optical Coherence and Quantum Optics* (Cambridge University Press, Cambridge, England, 1995).
[2] U. Leonhardt, *Measuring the Quantum State of Light* (Cambridge University Press, Cambridge, England, 1997).
[3] D. Bouwmeester, A. Ekert, and A. Zeilinger, *The Physics of Quantum Information* (Springer-Verlag, Berlin, 2000).
[4] P. Kok, W. J. Munro, K. Nemoto, T. C. Ralph, J. P. Dowling, and G. J. Milburn, Rev. Mod. Phys. **79**, 135 (2007).
[5] A. Wallraff *et al.*, Nature (London) **431**, 162 (2004).
[6] R. J. Schoelkopf and S. M. Girvin, Nature (London) **451**, 664 (2008).
[7] A. Blais *et al.*, Phys. Rev. A **69**, 062320 (2004).
[8] O. Astafiev *et al.*, Science **327**, 840 (2010).
[9] M. A. Sillanpää *et al.*, Nature (London) **449**, 438 (2007).
[10] J. Majer *et al.*, Nature (London) **449**, 443 (2007).
[11] A. A. Houck *et al.*, Nature (London) **449**, 328 (2007).
[12] F. Deppe *et al.*, Nature Phys. **4**, 686 (2008).
[13] M. Mariantoni *et al.*, Phys. Rev. B **78**, 104508 (2008).
[14] T. Niemczyk *et al.*, Supercond. Sci. Technol. **22**, 034009 (2009).
[15] D. Bozyigit *et al.*, arXiv:1002.3738.
[16] F. Helmer, M. Mariantoni, E. Solano, and F. Marquardt, Phys. Rev. A **79**, 052115 (2009).
[17] G. Romero, J. J. García-Ripoll, and E. Solano, Phys. Rev. Lett. **102**, 173602 (2009).
[18] E. P. Menzel *et al.*, Phys. Rev. Lett. **105**, 100401 (2010).
[19] J. Gabelli *et al.*, Phys. Rev. Lett. **93**, 056801 (2004).
[20] R. Movshovich *et al.*, Phys. Rev. Lett. **65**, 1419 (1990).
[21] M. Mariantoni, Ph.D thesis, TU München, 2009.
[22] E. Tholen, Ph.D. thesis, KTH Stockholm, 2009.
[23] C. W. J. Beenakker and H. Schomerus, Phys. Rev. Lett. **86**, 700 (2001).
[24] R. E. Collin, *Foundations for Microwave Engineering* (Wiley-IEEE, New York, 2000), 2nd ed.
[25] C. M. Caves, Phys. Rev. D **26**, 1817 (1982).
[26] H. Nyquist, Phys. Rev. **32**, 110 (1928).